Electronic Supplementary Material (ESI) for New Journal of Chemistry.
This journal is © The Royal Society of Chemistry and the Centre National de la Recherche Scientifique 2017

Electronic Supporting information

Functionalized calix[4]arene as colorimetric dual sensor for Cu(II) and cysteine in aqueous media: Experimental and computational study

Madhuri Bhatt,[†,a,b] Debdeep Maity,[†,a] Vinayak Hingu,[a] Eringathodi Suresh,[a,b] Bishwajit Ganguly,*[a,b] and Parimal Paul*[a,b]

[a]Analytical Division and Centralized Instrument Facility,

[b]Academy of Scientific and Innovative Research (AcSIR); CSIR-Central Salt and Marine Chemicals Research Institute, G. B. Marg, Bhavnagar 364002, India

* Corresponding authors. Tel.: +91 278 2565180,

E-mail: ppaul@csmcri.org, ppaul@csmcri.res.in (P. Paul),

ganguly@csmcri.org, ganguly@csmcri.res.in (B. Ganguly).

Table of Content

S1. Synthesis of the intermediate compound C and D

The intermediate compound **C** and **D** was synthesized following literature procedure reported earlier from this laboratory.

Synthesis of compounds **C**

In a solution of calix[4]arene (B) (2 mmol) in freshly distilled acetone (80 mL), methylbromo acetate (5 mmol) and K_2CO_3 (2.5 mmol) were added and the reaction mixture was heated at reflux for 20 h under an inert atmosphere. The solution was then allowed to cool to room temperature and evaporated to dryness by rotary evaporation. The residue was then triturated three times with methanol (25 mL each time) and filtered off the white solid. The desired white solid was kept under high vacuum overnight. Compound C was synthesized from intermediate B following the modified literature method,[62] similar to that described for synthesis of D. Yield: 76%. IR, nmax(KBr pellet)/ cm^{-1} 3402 (OH), 1760 (CQO); ^{1}H NMR (200 MHz, CDCl3): d 7.55 (s, 2H, Ar OH), 7.04 (d, 4H, J = 7.4 Hz, Ar-Hm), 6.9 (d, 4H, J = 7.4 Hz, Ar-Hm), 6.77–6.61 (m, 4H, Ar-Hp), 4.74 (s, 4H, -OCH2CO-), 4.46 (d, 4H, J=13.2 Hz, ArCH2Ar), 3.87 (s, 6H, -CH3), 3.39 (d, 4H, J=13.2 Hz,ArCH2Ar). ESMS (m/z): found 591.54 (95%), calcd for [C + Na^+] 591.60; found 607.51 (100%), calcd for [C + K^+] 607.71. Anal calcd for $C_{34}H_{32}O_8$: calcd C, 71.81; H, 5.67%. Found: C, 71.67; H, 5.43%.

Synthesis of compounds **D**

In a solution of p-tert-butylcalix[4]arene (A) (2 mmol) in freshly distilled acetone (80 mL), methylbromo acetate (5 mmol) and K_2CO_3 (2.5 mmol) were added and the reaction mixture was heated at reflux for 20 h under an inert atmosphere. The solution was then allowed to cool to room temperature and evaporated to dryness by rotary evaporation. The residue was then triturated three times with methanol (25 mL each time) and filtered off the white solid. The desired white solid was kept under high vacuum overnight. Yield: 1.124 g (71%). IR, nmax(KBr pellet)/ cm1 3435 (OH), 1759 (CQO); ^{1}H NMR (200 MHz, CDCl3): d 7.03 (s, 4H, Ar-Hm), 6.98 (s, 2H, Ar-OH), 6.81 (s, 4H, Ar-Hm), 4.73 (s, 4H, -OCH_2CO), 4.43 (d, 4H, J = 13.2 Hz, ArCH2Ar), 3.85 (s, 6H, -CH_3), 3.32 (d, 4H, J = 13.2 Hz, ArCH2Ar), 1.27 (s, 18H, -$C(CH_3)_3$), 0.97 (s, 18H, -$C(CH_3)_3$). ESMS (m/z): found 831.31(100%), calcd for [D+K^+] 832.13. Anal calcd for $C_{50}H_{64}O_8$: calcd C, 75.72; H, 8.13%. Found: C,74.89; H, 7.95%.

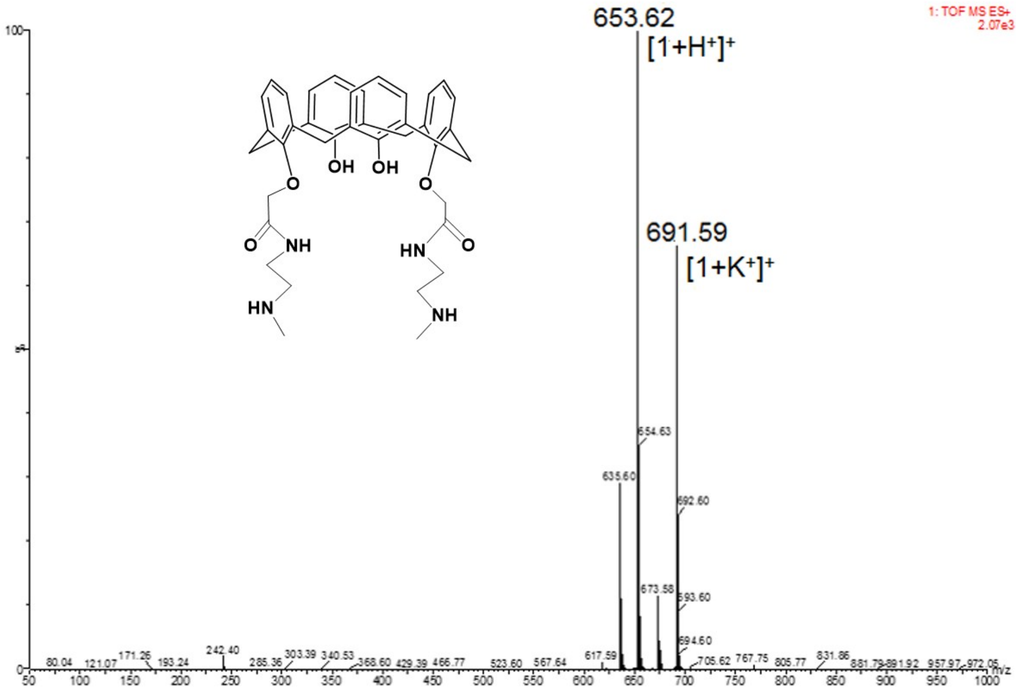

Fig. S2. Mass spectrum (ES-MS) of compound **1**

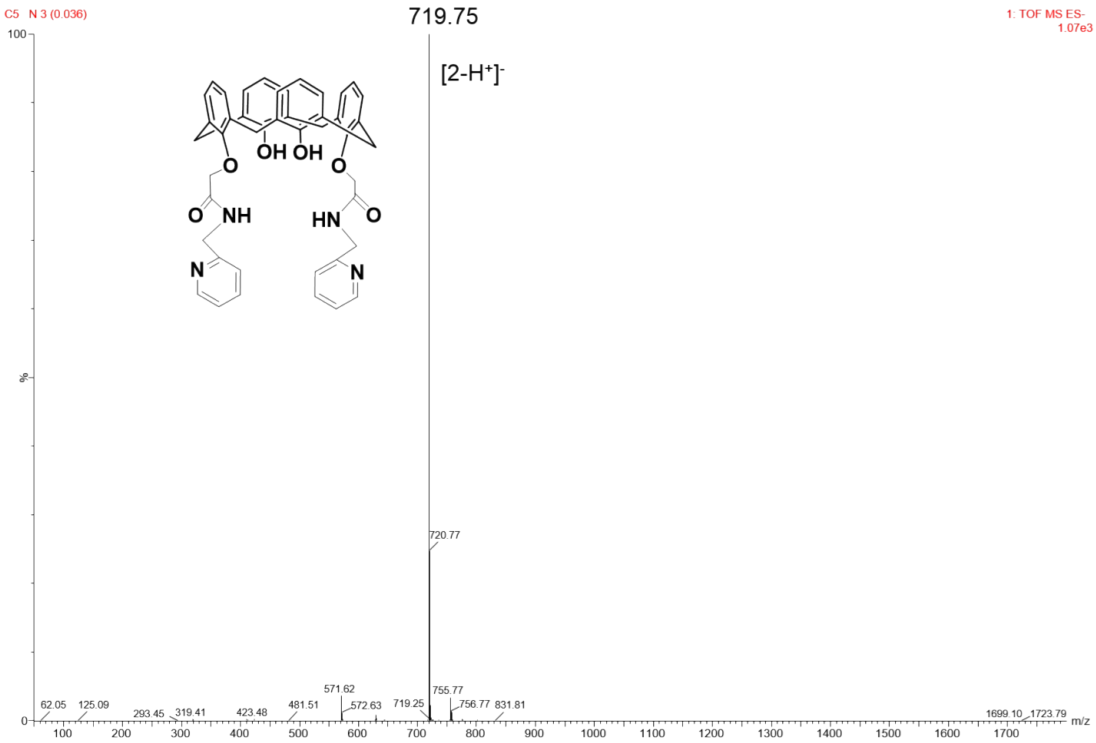

Fig. S3. Mass spectrum (ES-MS) of compound **2**

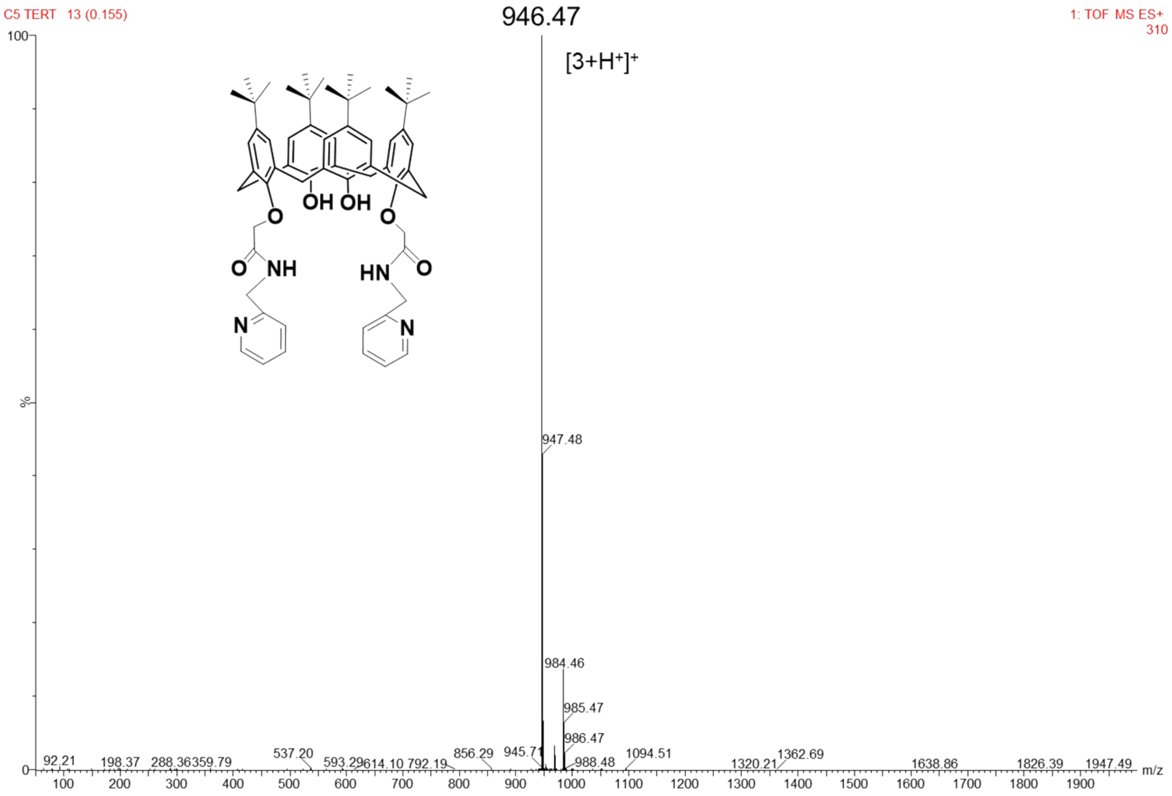

Fig. S4. Mass spectrum (ES-MS) of compound **3**

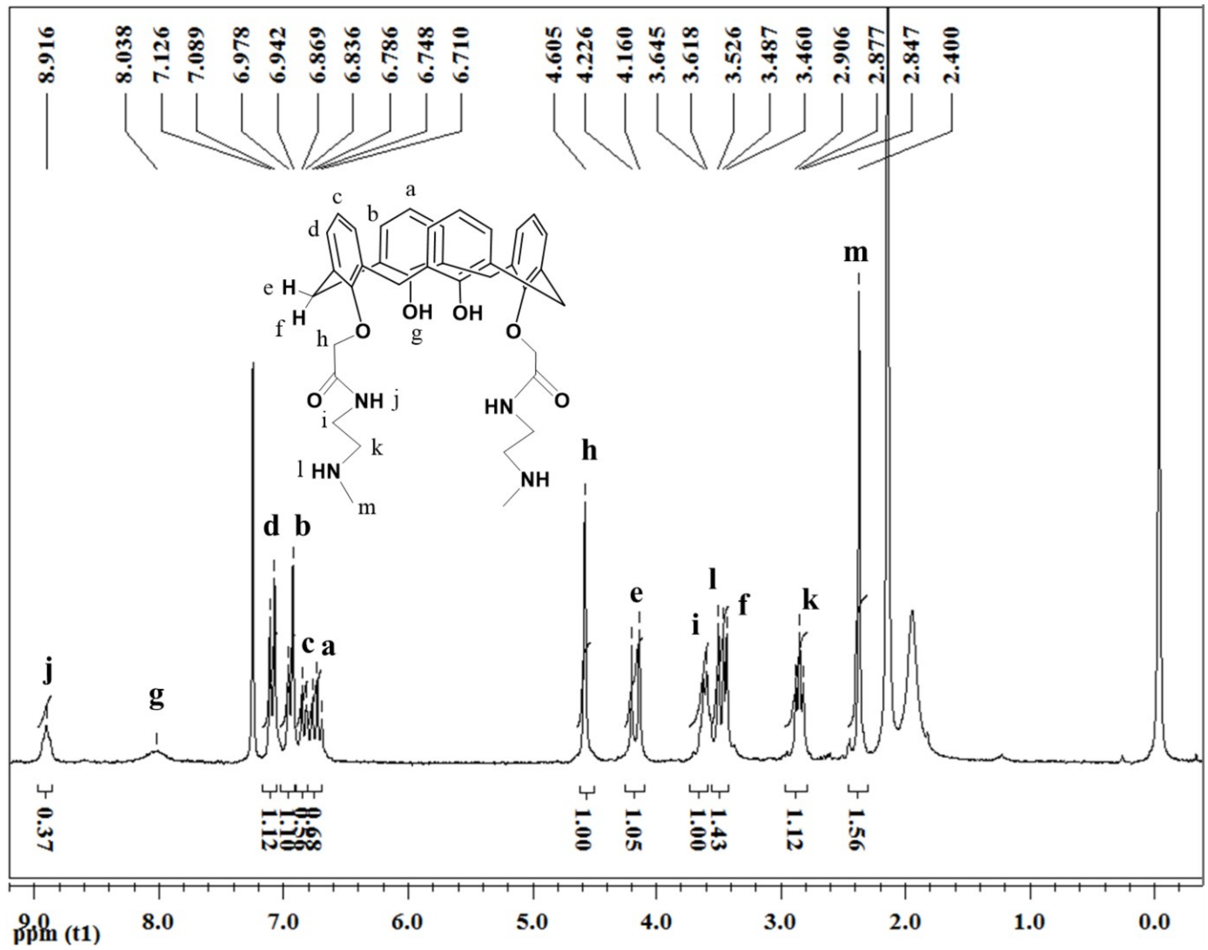

Fig. S5. ^{1}H NMR spectrum of compound **1**

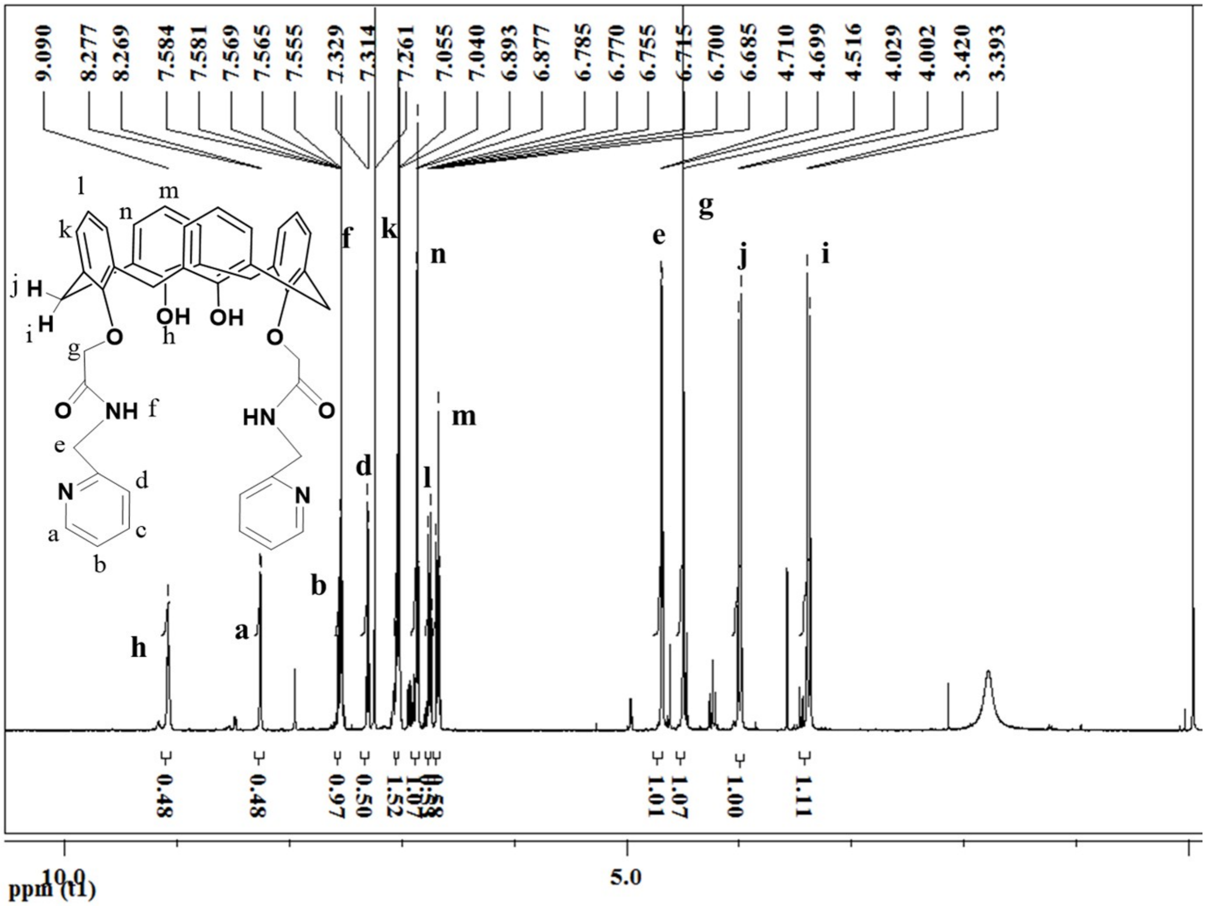

Fig. S6. ^{1}H NMR spectrum of compound **2**

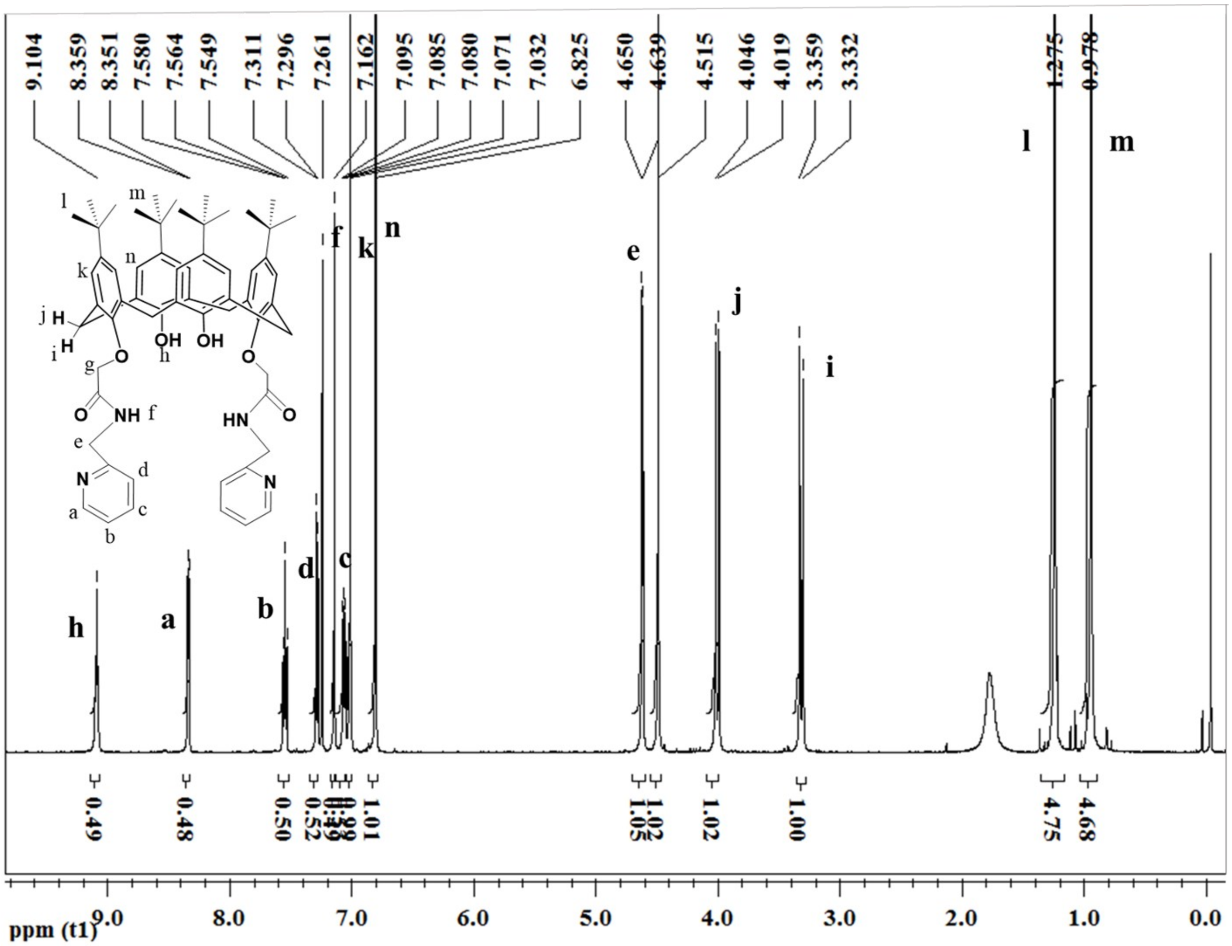

Fig. S7. ^{1}H NMR spectrum of compound **3**

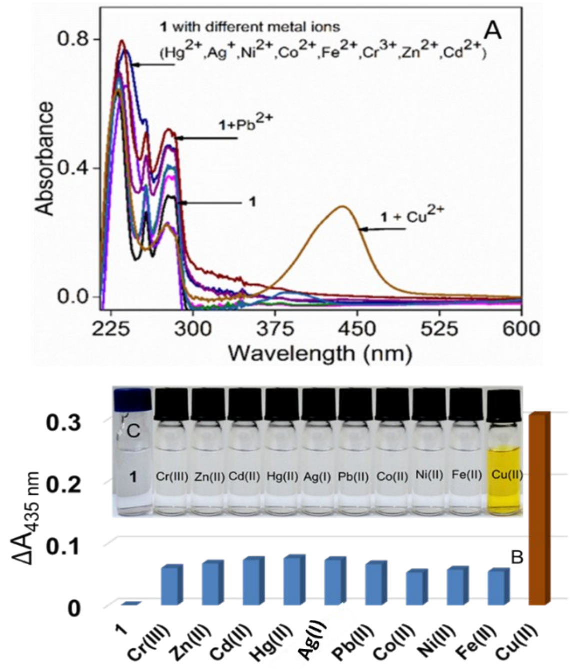

Fig. S8. (A) Absorption spectra of **1** (50 μM) in H_2O in presence of different cations (5 mM, 100 equiv respectively) is shown. (B) Absorbance change profile at 435 nm against different metal ions. (C) Corresponding colour changes upon addition of different metal ions are shown.

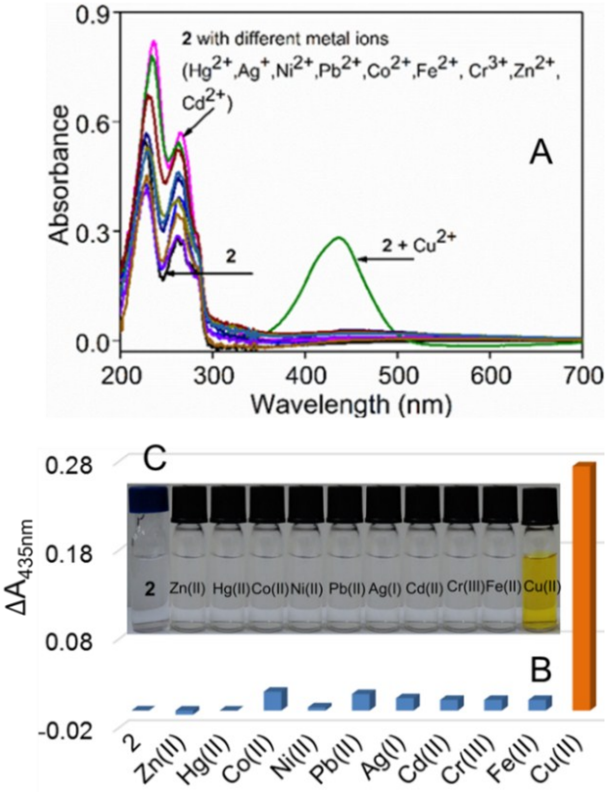

Fig. S9. (A) Absorption spectra of **2** (50 μM) in acetonitrile in presence of different cations (5 mM, 100 equivalent, respectively) is shown. (B) Absorbance change profile at 435 nm against different metal ions and (C) corresponding colour changes upon addition of different metal ions are shown.

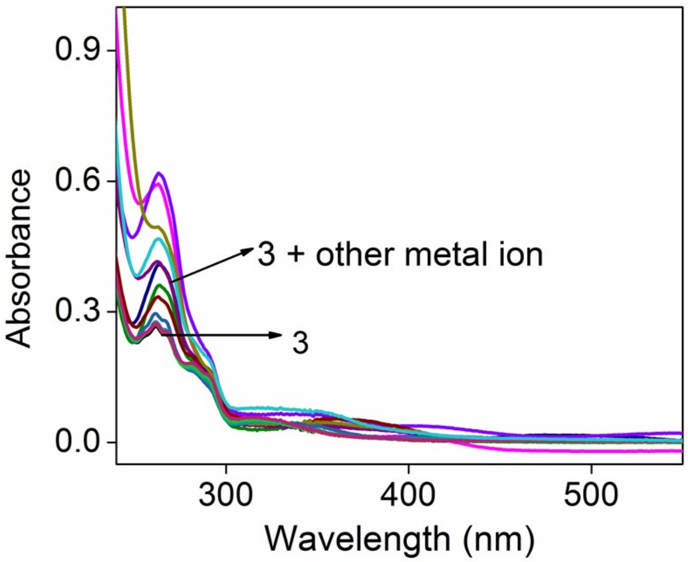

Fig. S10. UV-vis spectra of **3** (50 μM) in acetonitrile in presence of different metal ions (100 fold excess) is shown.

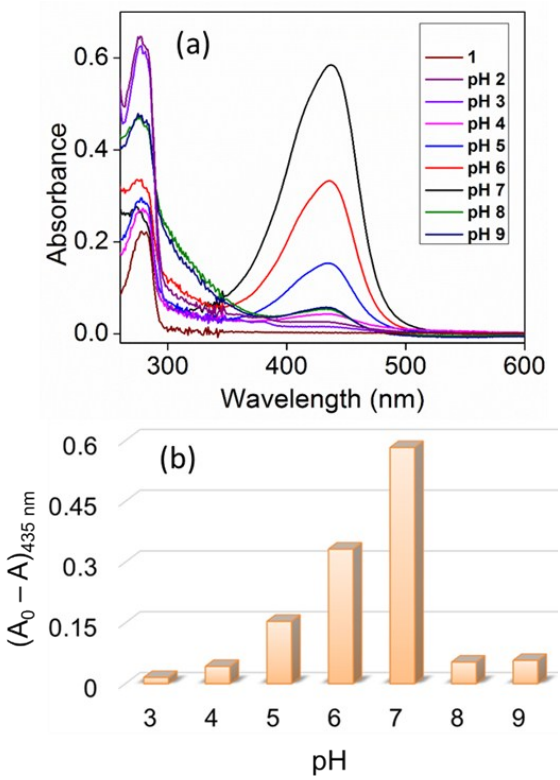

Fig. S11. (a) UV-vis spectra of **1** after addition of Cu^{2+} at different pH in water: acetonitrile (1:1) (b) Bar diagram showing the change in absorbance of **1** after addition of Cu^{2+} at different pH in H_2O: acetonitrile (1:1)

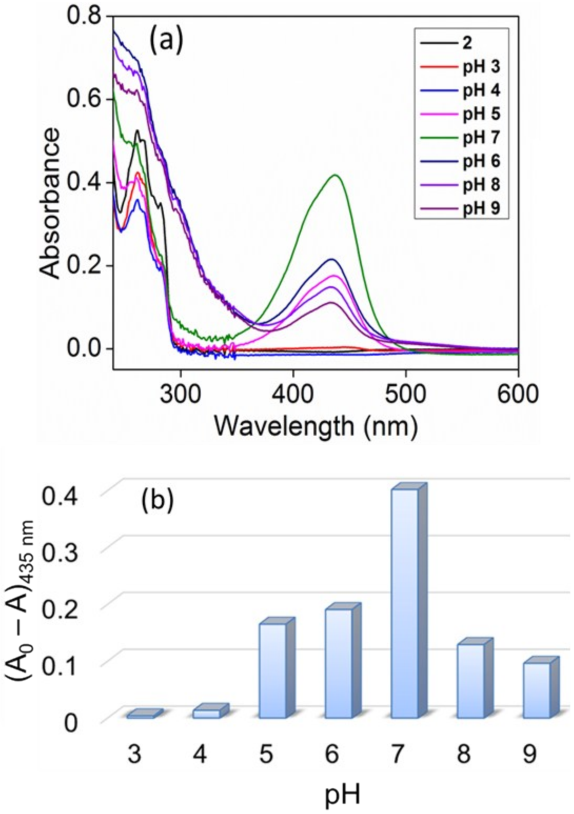

Fig. S12. (a) UV-vis spectra of **2** after addition of Cu^{2+} at different pH in water: acetonitrile (1:1) (b) Bar diagram showing the change in absorbance of **2** after addition of Cu^{2+} at different pH in H_2O: acetonitrile (1:1)

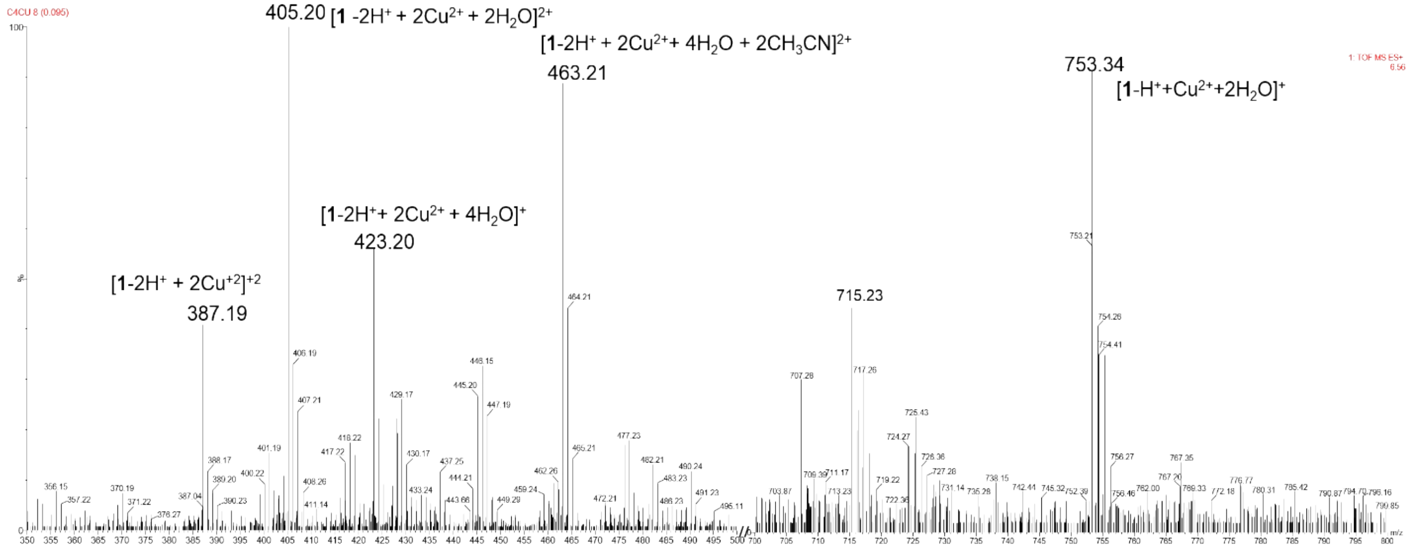

Fig. S13. Mass spectrum of **1** with Cu^{2+}

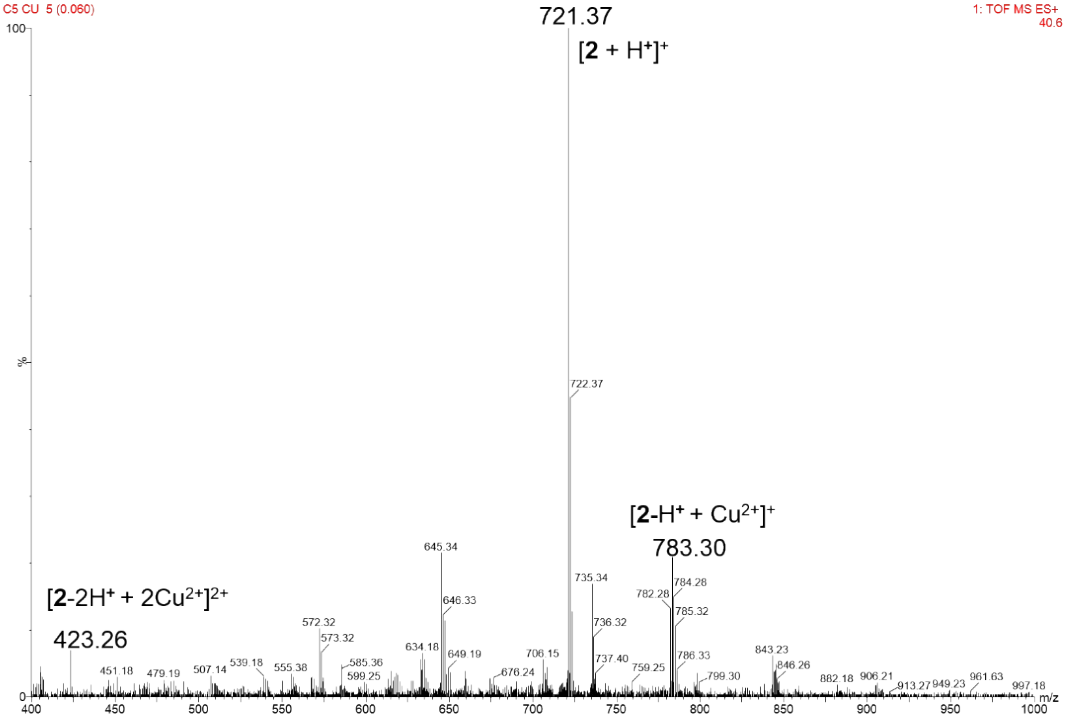

Fig. S14 Mass spectrum of **2** with Cu^{2+}

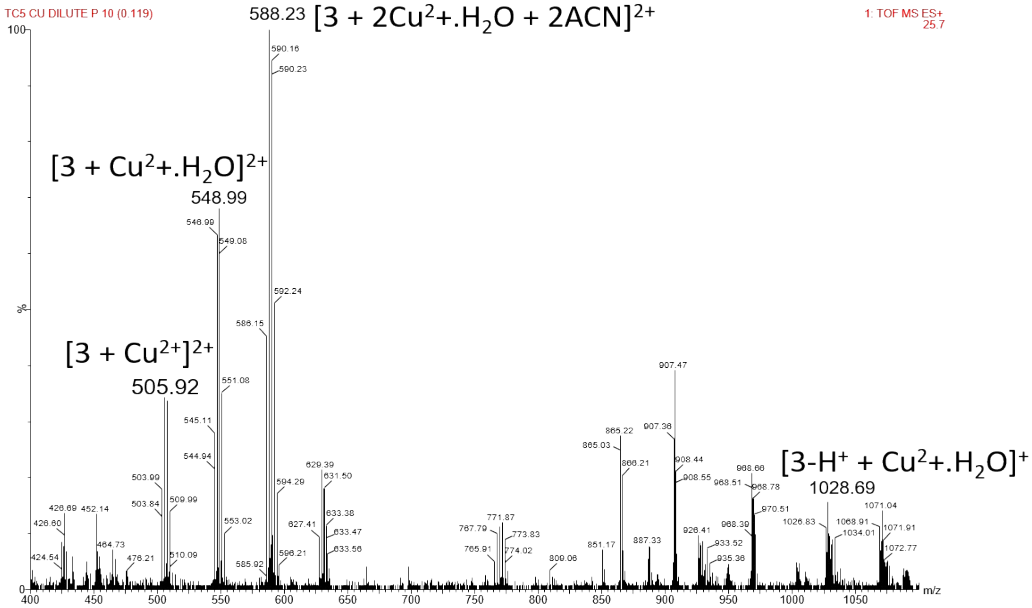

Fig. S15. Mass spectrum of **3** with Cu^{2+}

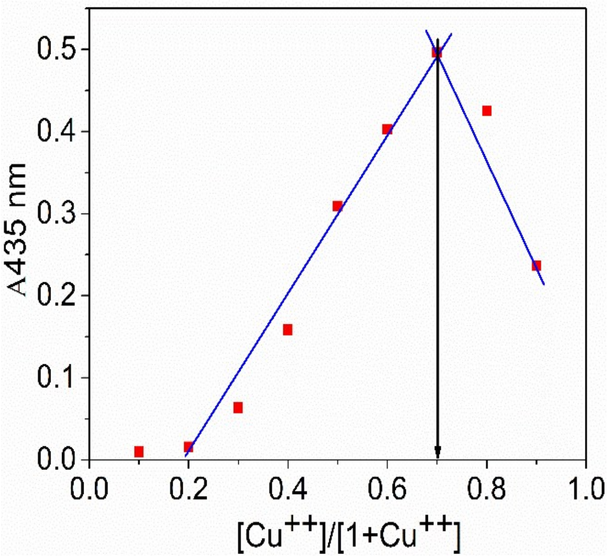

Fig. S16. Job's plot of **1** is shown with Cu^{2+} in acetonitrile. The total concentration of **1** and Cu^{2+} is set at 100 μM.

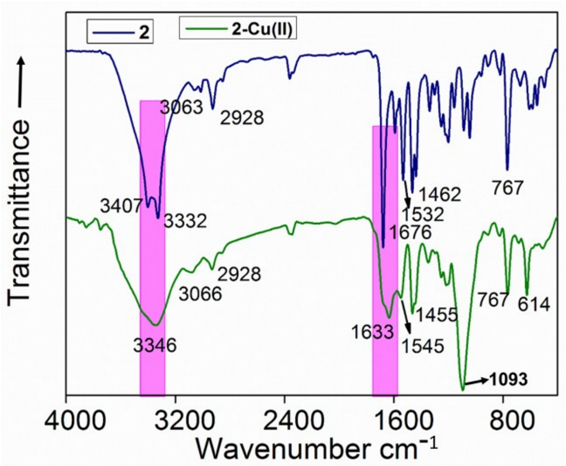

Fig. S17. FT-IR spectral change of **2** and **2**-Cu^{2+}

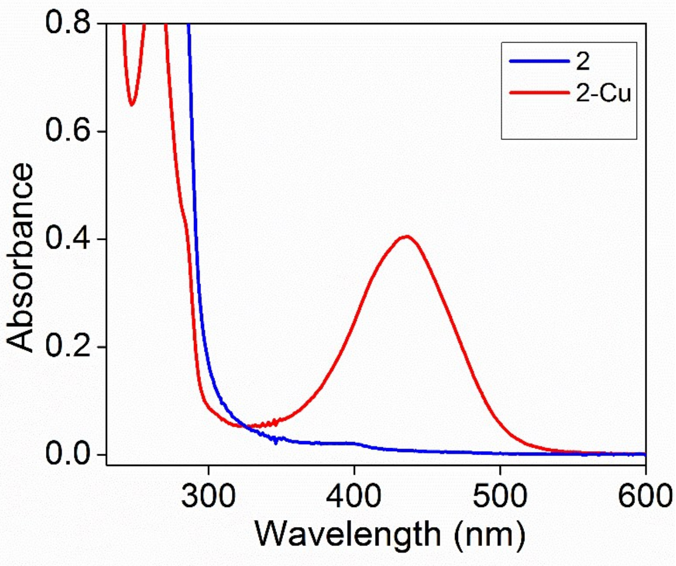

Fig. S18 UV-vis spectra of **2** and solid complex of **2**-Cu^{2+} in acetonitrile

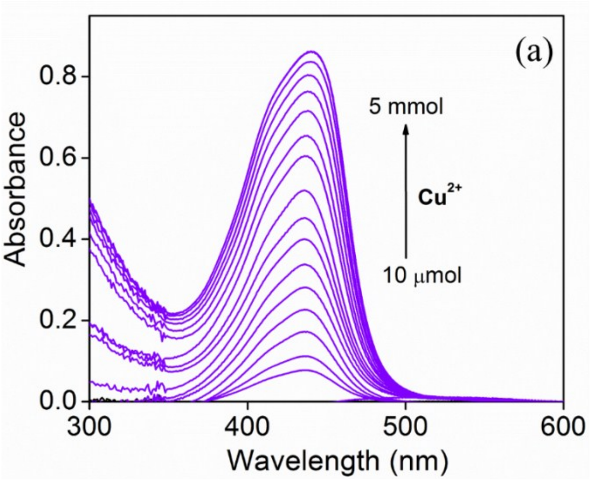
(a)
5 mmol
Cu2+
10 μmol
Absorbance
0.0
0.2
0.4
0.6
0.8
300
400
500
600
Wavelength (nm)

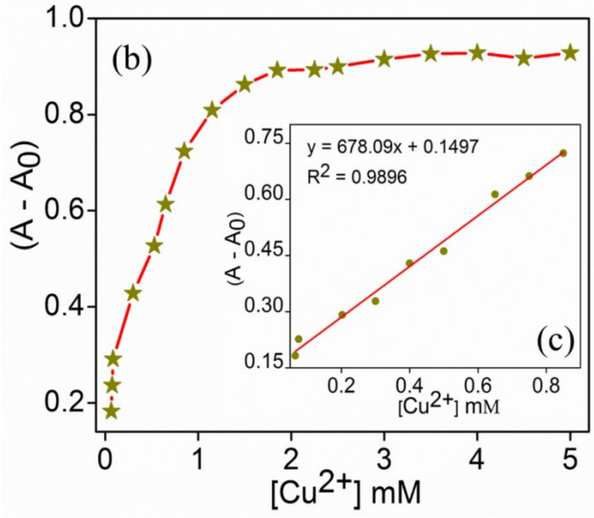
(b)
(A - A0)
0.2
0.4
0.6
0.8
1.0
0
1
2
3
4
5
[Cu2+] mM
y = 678.09x + 0.1497
R2 = 0.9896
(c)
(A - A0)
0.15
0.30
0.45
0.60
0.75
0.2
0.4
0.6
0.8
[Cu2+] mM

Fig. S19. UV-Vis spectral changes for **1** (25 μM) in acetonitrile-H_2O (1:) upon addition of incremental amount of Cu^{2+} (10 μM to 5 mM), (b) changes in the absorbance at 435 nm with incremental addition of Cu^{2+} and (c) linear fit up to 1.0 mM.

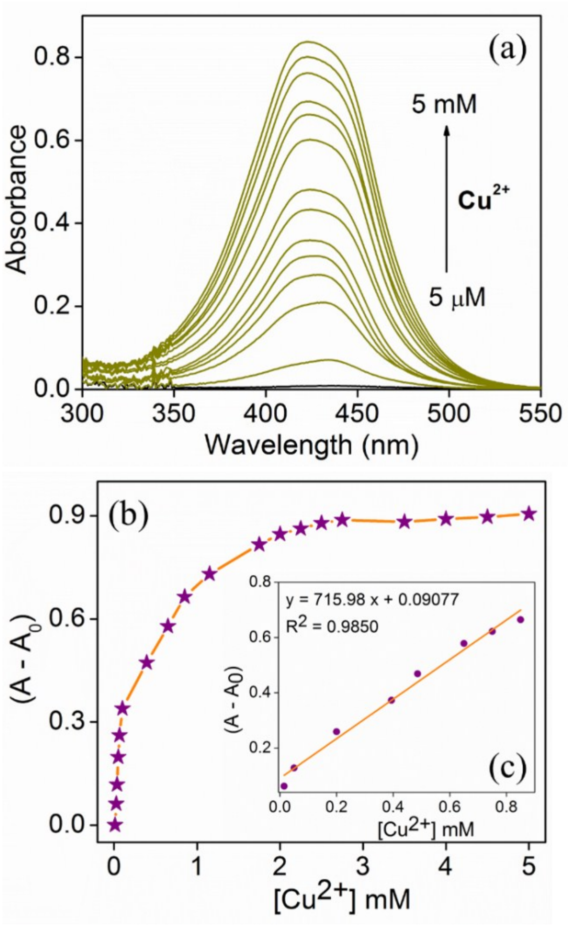

Fig. S20. UV-Vis spectral changes for **2** (50 μM) in acetonitrile upon addition of incremental amount of Cu^{2+} (5 μmol to 5 mmol), (b) changes in the absorbance at 435 nm with incremental addition of Cu^{2+} and (c) linear curve calculation of **2** at 435nm. All the spectral data were recorded in acetonitrile media.

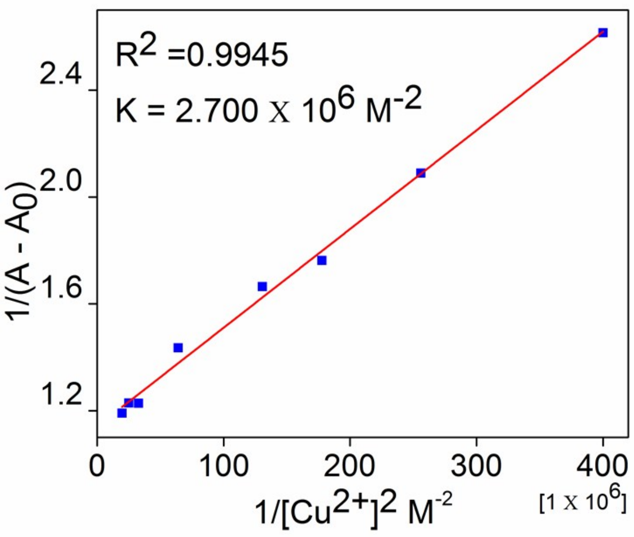

Fig. S21. Benesis-Hildebrand plot (435 nm absorbance) of **1**, with 1:2 stoichiometry for complexation between **1** and Cu^{2+} in acetonitrile.

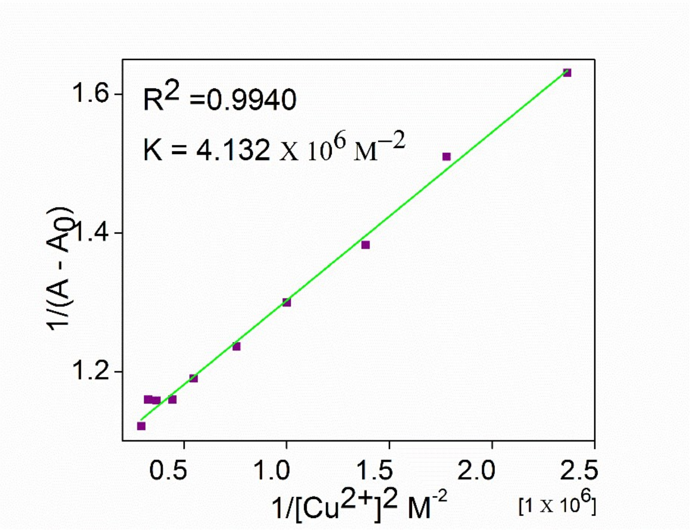

Fig. S22. Benesis-Hildebrand plot (435 nm absorbance) of **1**, with 1:2 stoichiometry for complexation between **1** and Cu^{2+} in H_2O

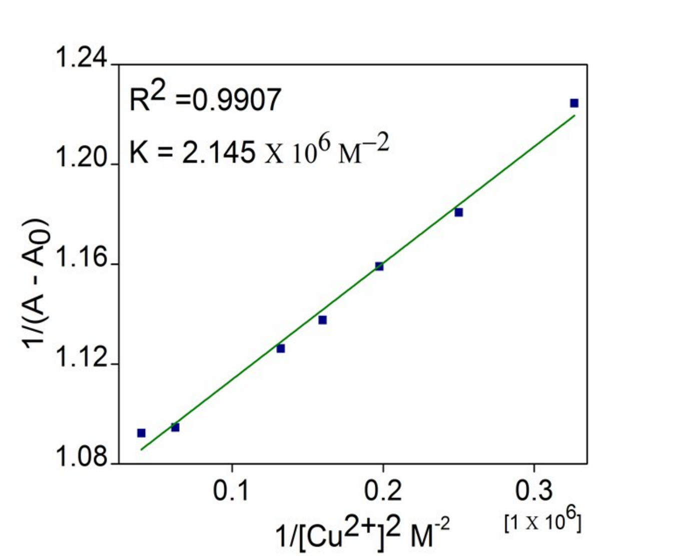

Fig. S23. Benesis-Hildebrand plot (435 nm absorbance) of **2**, with 1:2 stoichiometry for complexation between **2** and Cu^{2+} in acetonitrile.

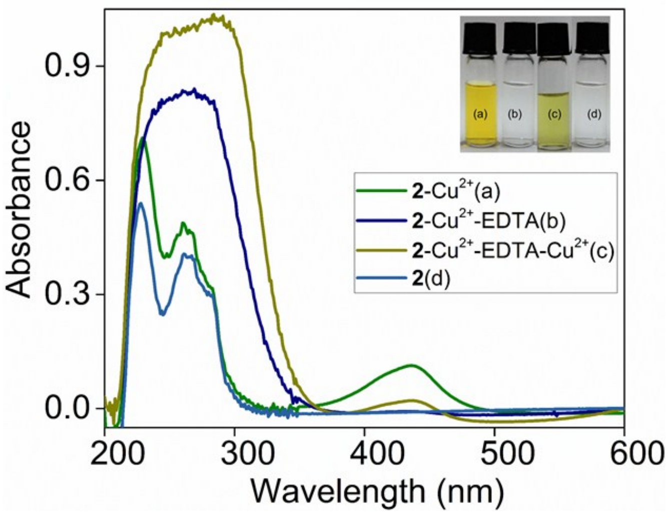

Fig. S24. UV-vis spectral change of **2** is shown upon addition of Cu^{2+} and then EDTA and Cu^{2+} again to investigate reversibility in acetonitrile-H_2O.

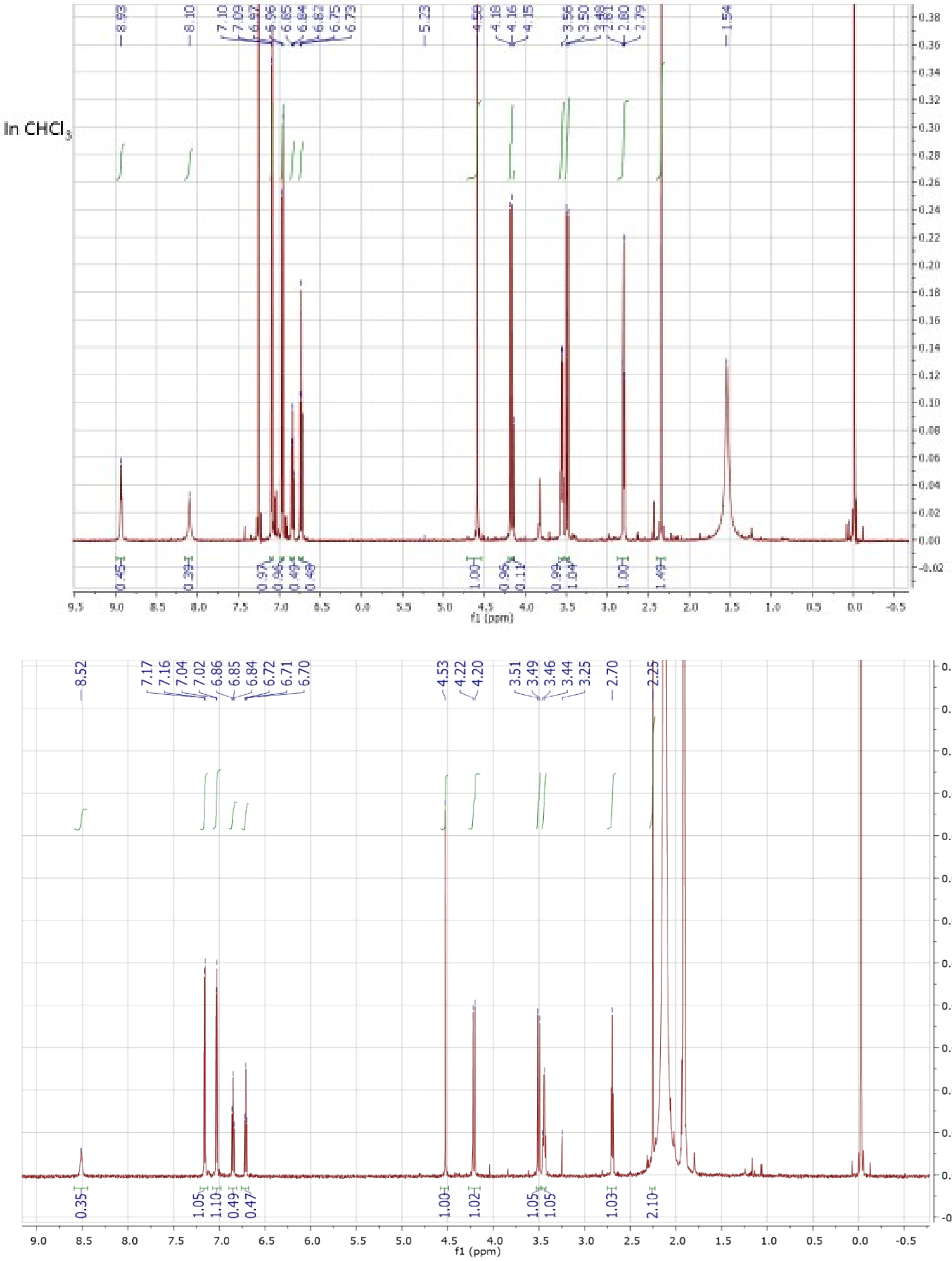

Fig. S25. ^{1}H NMR spectra of compound **1** in $CDCl_3$ (top) and CD_3CN (bottom), recorded in 600 MHz instrument (JEOL)

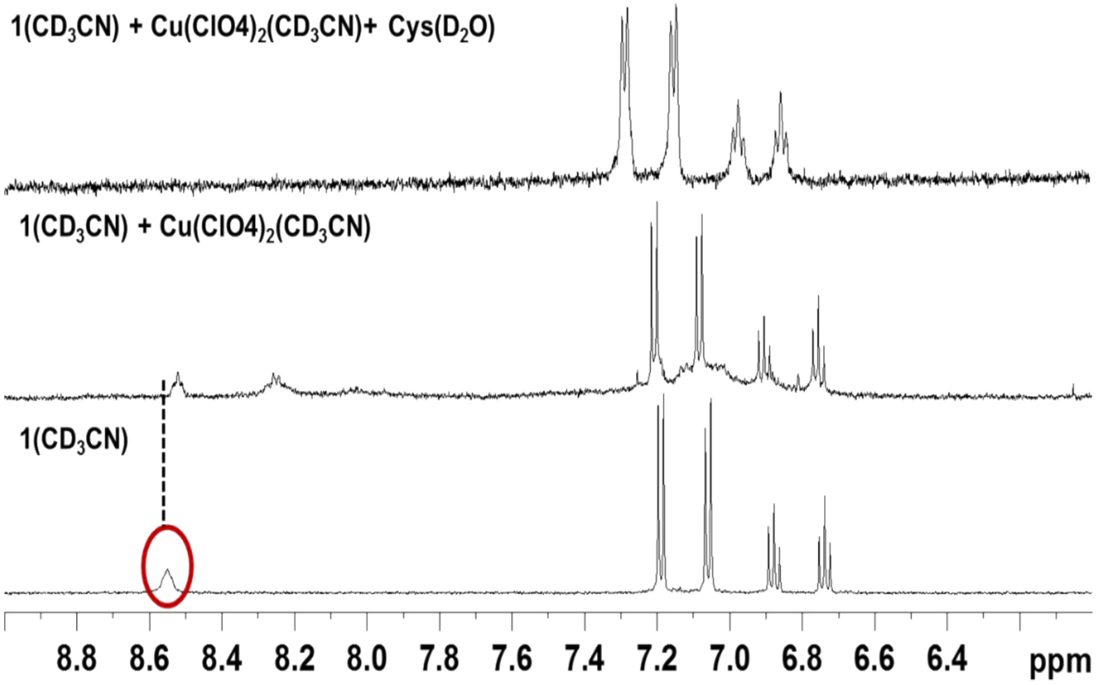

Fig. S26. ^{1}H NMR spectra (partial view) of compound **1** in CD_3CN (bottom) and the same upon addition of $Cu(ClO_4)_2$ and Cysteine dissolved in D_2O.

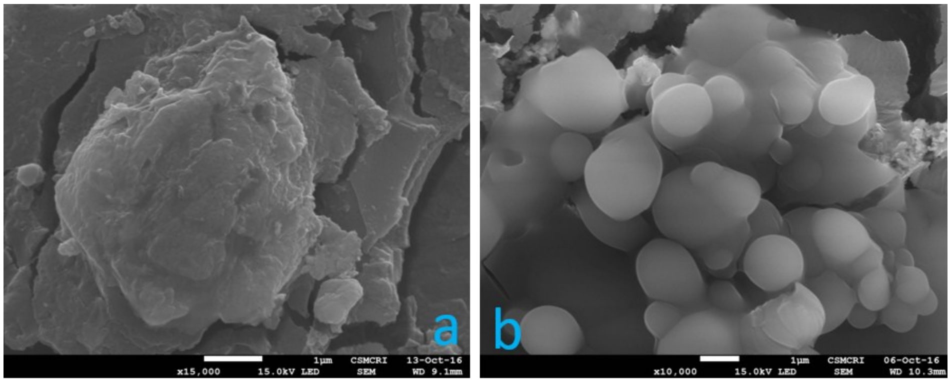

Fig. S27 FE-SEM images of compound **2** (a) and its Cu^{2+} complex (b)